Comparative reservoir competence of *Peromyscus leucopus* and mouse models for *Borrelia burgdorferi* B31

Short Title: *Peromyscus leucopus* and mouse model reservoir competence for *B. burgdorferi*

Jeffrey S. Bourgeois[1,2], Stephanie S. You[1,2], Luke H. Clendenen[1,2], Muskan Shrestha[1,2], Tanja Petnicki-Ocwieja[1,2], Sam R Telford III[2,3], Linden T. Hu[1,2,#]

1. Tufts University, Department of Molecular Biology and Microbiology, Boston, MA, United States of America
2. Tufts University, Tufts Lyme Disease Initiative, Boston, MA, United States of America
3. Tufts University, Department of Infectious Disease and Global Health, Tufts University, North Grafton, MA, United States of America

Corresponding Author: linden.hu@tufts.edu

Abstract

The Lyme disease spirochete *Borrelia burgdorferi* drives a range of acute and chronic maladies in humans and other incidental hosts infected with the pathogen. However, a primary vertebrate reservoir, *Peromyscus leucopus* appears spared from any symptomology following infection. This has led to a common assumption that *P. leucopus* and *B. burgdorferi* exist symbiotically: *P. leucopus* restrain their immune response against the microbe and enable the enzootic cycle while *B. burgdorferi* avoids causing damage to the host. While aspects of this hypothesis have been tested, the exact interactions that occur between *P. leucopus* and *B. burgdorferi* during infection remain largely unknown. Here we compared infection of *P. leucopus* with *B. burgdorferi* with infection of the traditional *B. burgdorferi* murine models—C57BL/6J and C3H/HeN *Mus musculus*, which develop signs of inflammation akin to human disease. We find that in contrast to our expectations, *B. burgdorferi* were able to reach much higher burdens in *M. musculus*, and that the overall kinetics of infection differed between the two rodent species. Surprisingly, we also found that *P. leucopus* remained infectious to larval *Ixodes scapularis* for a far shorter period than either *M. musculus* strain. In line with these observations, we found that *P. leucopus* does launch a modest but sustained inflammatory response against *B. burgdorferi* in the skin, which we hypothesize leads to reduced bacterial viability and infectivity in these hosts. These observations provide new insight into the nature of reservoir species and the *B. burgdorferi* enzootic cycle.

Author Summary

The bacteria that causes Lyme disease, *Borrelia burgdorferi*, must alternate between infecting a vertebrate host—usually rodents or birds—and ticks. In order to be successful in that endeavor the bacteria must avoid being killed by the vertebrate host before it can infect a new larval tick. In this work we examine how *B. burgdorferi* and one of its primary vertebrate reservoirs, *Peromyscus leucopus*, interact during an experimental infection and find contrary to expectations *B. burgdorferi* appear to colonize its natural host worse than conventional lab mouse models. These data question long-held assumptions about *P. leucopus* immunology and could potentially serve as a foundation to uncover ways to disrupt the spread of *B. burgdorferi* in nature.

Keywords

Peromyscus leucopus, Borrelia burgdorferi, Borreliella burgdorferi, Lyme disease, Ixodes scapularis, vector-borne disease, enzootic cycle

Introduction

Few endemic pathogens in the United States are as infamous as *Borrelia burgdorferi* sensu stricto (also called *Borreliella burgdorferi*), or the "Lyme disease spirochete," which causes a range of drive acute and chronic symptomology in humans. In North America, *B. burgdorferi* is spread between vertebrate hosts by the "deer tick" or "black-legged tick" *Ixodes scapularis* [1-3]. This enzootic cycle occurs ad infinitum as larval ticks collect *B. burgdorferi* from infected vertebrates, molt, transmit the infection to new vertebrate hosts as nymphal ticks, molt, and produce new larval ticks [4]. While *B. burgdorferi* is found in numerous permissive vertebrate hosts ranging from birds [5] to dogs [6], one of the dominant North American reservoir host for *B. burgdorferi* is the white-footed mouse *Peromyscus leucopus* [7] which, by some estimates, accounts for ~30% of *B. burgdorferi* spread into larval ticks [8], though the exact value likely varies by region and year. This aligns with other work which noted that in endemic regions, up to ~30-95% of this highly abundant rodent are infected with *B. burgdorferi* [9, 10]. Numerous ecological and laboratory studies have noted a unique relationship between *B. burgdorferi* and *P. leucopus* as, outside of neonate infection [11], *B. burgdorferi* has no detectable impact on *P. leucopus* fitness [10] and does not drive any observed behavioral [12, 13] or histological [11] changes. Even at the molecular level, two studies found very few changes to transcript abundance during post-acute infection (4-5 weeks post infection) [14, 15]. This apparent limited immune response occurs despite considerable evidence that *P. leucopus* remain colonized by *B. burgdorferi* for months following infection [10, 16]. This has led to a dominating hypothesis in the field that *P. leucopus* and the Lyme disease spirochete appear to exist in a sort of truce throughout the infection: *P. leucopus* does not try to eradicate the pathogen following infection and in return *B. burgdorferi* itself does not cause any detectable damage. While this hypothesis is well-grounded in parasitism theory, as long co-existence between parasites and hosts are often thought to result in mutualism [17], the extent to which this symbiosis occurs between *P. leucopus* and *B. burgdorferi* has not been thoroughly tested.

Here we seek to better define the relationship between *P. leucopus* and *B. burgdorferi* by examining host and bacterial dynamics throughout infection. We compare *B. burgdorferi* burden dynamics in *P. leucopus* as well as two inbred *Mus musculus* mouse strains (C57BL/6J and C3H/HeN) and find that *P. leucopus* restrain *B. burgdorferi* burden compared to the lab mice. This correlates with a modest transcriptional burst of genes associated with innate and adaptive immunity in the skin, suggesting that *P. leucopus* are actively responding to and restricting *B. burgdorferi* infection. Notably, *P. leucopus* also transmit the pathogen to *I. scapularis* larvae at substantially lower rates and for a much shorter amount of time than lab mice. Together, these data do not support a narrative of a highly evolved mutualistic relationship between *P. leucopus* and *B. burgdorferi* to promote *B. burgdorferi* fitness, but instead suggest that *B. burgdorferi* may have evolved with tick feeding cycles to take advantage of a short window where *P. leucopus* are permissive enough to support the enzootic cycle.

Results

Inbred *Peromyscus leucopus* restrict *Borrelia burgdorferi* during early infection.

Substantial work has demonstrated that *P. leucopus* respond to the bacterial pathogen associated molecular pattern lipopolysaccharide (LPS) to a far lesser extent than inbred [18] and outbred [19] *M. musculus.* While *B. burgdorferi* lacks LPS, if bacterial sensing is broadly suppressed in *P. leucopus* this could enable *B. burgdorferi* to thrive until it can be collected during another tick bloodmeal. To test whether *P. leucopus* is more tolerant to *B. burgdorferi* during early

infection, we injected inbred *P. leucopus* and two inbred *M. musculus* strains (C57BL/6J and C3H/HeN) subcutaneously with $1x10^5$ *B. burgdorferi* B31 spirochetes and collected skin from the injection site one week later. Note that these *M. musculus* strains were chosen because they have routinely been used in the *B. burgdorferi* field to mimic severe (C3H strains) and moderate (C57BL/6J) Lyme disease [20], and thus much of our understanding of murine *B. burgdorferi* infection are derived from these strains. Further, these inbred mice pair well with our inbred *P. leucopus* model. We hypothesized that if *P. leucopus* are highly permissive to *B. burgdorferi*, the microbe would be able to reach higher bacterial burdens than in *M. musculus*. Curiously, while we were able to culture spirochetes from the injection site of all the tested rodents **(Figure 1A)**, we found that *P. leucopus* had equal bacterial burdens (measured by digital droplet PCR [ddPCR]) at the injection site as C57BL/6J mice but substantially lower bacterial burden compared to C3H/HeN mice **(Figure 1B)**. This suggests that, if anything, *P. leucopus* are less permissive to *B. burgdorferi* than inbred *M. musculus*.

While the *B. burgdorferi* subcutaneous injection model offers many advantages, it does not always accurately recapitulate wild infection where *I. scapularis* deliver a small number of *B. burgdorferi* and saliva proteins into the host during the bloodmeal. In order to better replicate natural infections, we repeated our above experiment except we placed five infected *I. scapularis* nymphs on the backs of *P. leucopus* and *M. musculus* before harvesting the tick bite site one week later. Again, we successfully cultured spirochetes out of all of the bite sites **(Figure 1C)**, but this time we found that *P. leucopus* had substantially (~100x) lower bacterial burdens at the bite site compared to either C57BL/6J or C3H/HeN mice **(Figure 1D)**. Thus, we conclude that despite being the proposed primary vertebrate host for *B. burgdorferi* and *I. scapularis* in North America [7]*, P. leucopus* is far less permissive to high *B. burgdorferi* burdens immediately following tick bite.

To understand the long-term impacts of this apparent growth restraint in *P. leucopus* we infected more rodents with *B. burgdorferi* via *I. scapularis* nymph placement and tracked bacterial burdens in individual mice over time by taking weekly ear punches over one month. We found that similar to our findings at the tick bite site *P. leucopus* had reduced bacterial burdens at early time points compared to the *M. musculus* strains **(Figure 1E)**. Curiously, we note that while both *M. musculus* strains had their peak infection at approximately 2.5 weeks post-nymph placement, we did not observe substantial increases in bacterial burdens in *P. leucopus* until 3.5-4.5 weeks post-nymph placement. This demonstrated not only that *P. leucopus* also appears to restrict *B. burgdorferi* growth in this secondary skin site, but that the overall infection kinetics in *P. leucopus* are substantially different than in the model species ($p_{rodent\ x\ time}$= 0.05, Two-Way ANOVA).

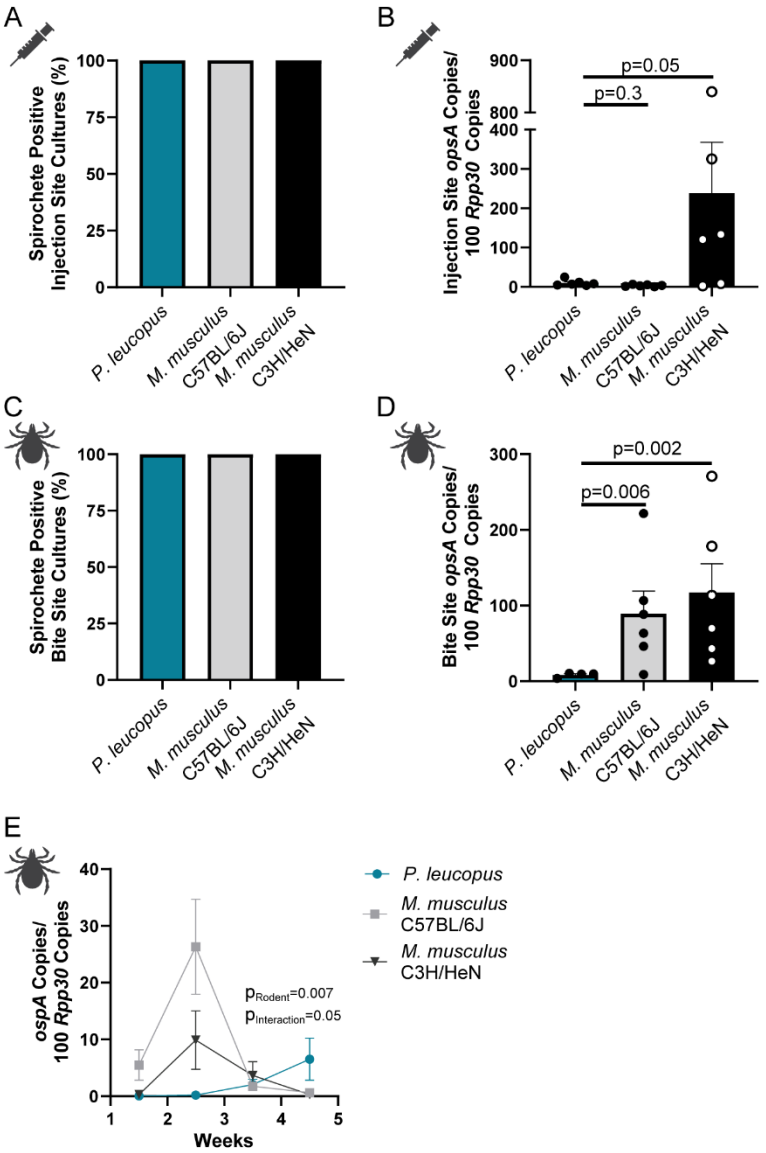

Figure 1: *B. burgdorferi* expand to greater numbers in *M. musculus* than in *P. leucopus* following tick bite. (A) *B. burgdorferi* are able to be cultured from needle injection sites from *P. leucopus* and *M. musculus* (n=6) one week post injection. (B) *B. burgdorferi* are present at substantially lower numbers at the needle injection site in *P. leucopus* than C3H/HeN mice by ddPCR. For panels A and B rodents were injected with 100,000 *B. burgdorferi* in 200µL of BSK-II via subcutaneous injection. (C) *B. burgdorferi* are able to be cultured from tick bite sites one week post infestation. (D) *B. burgdorferi* are present at substantially lower numbers at the tick bite site in *P. leucopus* (n=4) than C57BL/6J (n=6) or C3H/HeN (n=6) one week post infestation by ddPCR. For panels A and B, five infected nymphal *I. scapularis* were placed in a tick containment chamber on each rodent's back. The space under the containment chamber was harvested one week post infestation. For panels A and C, cultures were monitored for three weeks for spirochetes. For Panels B and D, data are normalized to copies of the mammalian *Rpp30* gene and p-values are generated by one-way ANOVA on log transformed data with Dunnett's multiple comparison test. For panels A-D, all rodents were between 8-12 weeks old at time of infection and both sexes are present. Bars represent the mean, dots represent individual mice, and error bars represent the standard error of the mean. (E) *B. burgdorferi* has different population dynamics in ear tissue from *P. leucopus* or *M. musculus* (n=3) following tick bite. Five infected nymphal *I. scapularis* were placed on a tick containment chamber on

each rodent's back and ear punches were taken weekly starting at 1.5 weeks post tick placement for ddPCR analysis. P-values generated by two-way ANOVA. For panel E, only male mice were used and all *M. musculus* were between 8 and 12 weeks old at time of infection while *P. leucopus* were estimated to be equal to or less than six months old. For all panels, data are pooled from two independent experiments.

Examining *B. burgdorferi* and *P. leucopus* interactions over time

In order to better understand how *P. leucopus* and *B. burgdorferi* influence each other over the course of infection we infested 20 *P. leucopus* with infected nymphs and 4 *P. leucopus* with uninfected nymphs across two independent experiments. Each rodent was euthanized at one of five terminal timepoints (1-, 2-, 4-, 8-, or 13-weeks post infestation, two rodents euthanized per timepoint per experiment) to obtain ear, joint, and heart tissue for microbiological, genomic and transcriptomic analysis **(Figure 2A)**. Mice infested with uninfected nymphs were harvested one week post placement. Additionally, each infected mouse was subjected to up to one intermediate timepoint (1-, 2-, 4-, 10-weeks post infestation) in which an ear punch was taken from a living mouse prior to infestation with larval ticks in order to assess the ability to pass infection onto new *I. scapularis*. These timepoints were chosen for two reasons: First, *P. leucopus* have a median lifespan of ~6 months in nature [10], and thus using 2–3 month-old *P. leucopus* and monitoring their infection for an additional 13 weeks likely captures all the physiologically relevant stages of rodent development. Second, the spring *I. scapularis* nymphal peak when many *P. leucopus* first get infected and the summer larval peak where larvae can acquire the infection are separated by about 1-3 months [21-23], and thus this captures the most important period of time that *B. burgdorferi* must exist in *P. leucopus* during the enzootic cycle.

To contextualize these results, we repeated these timecourses with C57BL/6J and C3H/HeN *M. musculus*. However, it should be noted that due to logistical constraints, these timecourses were completed separately and thus caution should be used when directly comparing the *P. leucopus* and *M. musculus* data.

***B. burgdorferi* fitness and bacterial burden are uncoupled in *P. leucopus*.**

At each terminal timepoint, we attempted to culture spirochetes out from approximately one half of a rodent ear in BSK-II. Surprisingly, we were unable to culture *B. burgdorferi* from *P. leucopus* until late in the infection, though still only approximately half of the cultures at these timepoints yielded living spirochetes **(Figure 2B)**. This contrasts with our studies with lab mice in which *B. burgdorferi* were readily cultured from ears at two weeks post infestation and we remained ≥50% successful in culturing spirochetes for the remainder of the experiment **(Figure 2C)**. Notably, using a ddPCR threshold of 1 copy of *ospA* per 10,000 copies of *Rpp30*, we observed similar dynamics in the rate at which we were able to detect molecular evidence of infection in the rodents **(Figures 2D, 2E)**. However, quantification of bacterial burdens corroborated our previous observations **(Figure 1E)** in that *P. leucopus* had a very modest spike in bacterial burden at four weeks post infestation **(Figure 2F)** while both lab mouse strains had substantially higher peaks at two weeks post infestation **(Figure 2G)**. Interestingly, while the quantified *B. burgdorferi* burden roughly correlated with our ability to culture spirochetes from ear cultures in both C57BL/6J and C3H/HeN mice, the same correlation did not exist with *P. leucopus*. In fact, we were not able to culture spirochetes from ear cultures at four weeks post infestation when ddPCR levels peaked but were able to culture at eight weeks when burden subsided by ddPCR. One possible explanation is that in *P. leucopus*, but not *M. musculus*, there is an accumulation of dead or non-culturable spirochetes for the first month of infection and that overall

bacterial fitness of the small remaining *B. burgdorferi* population improves thereafter. Together these data confirm and expand our conclusions from Figure 1, specifically that *P. leucopus* appear to harbor smaller numbers of *B. burgdorferi* in skin relative to inbred *M. musculus* strains.

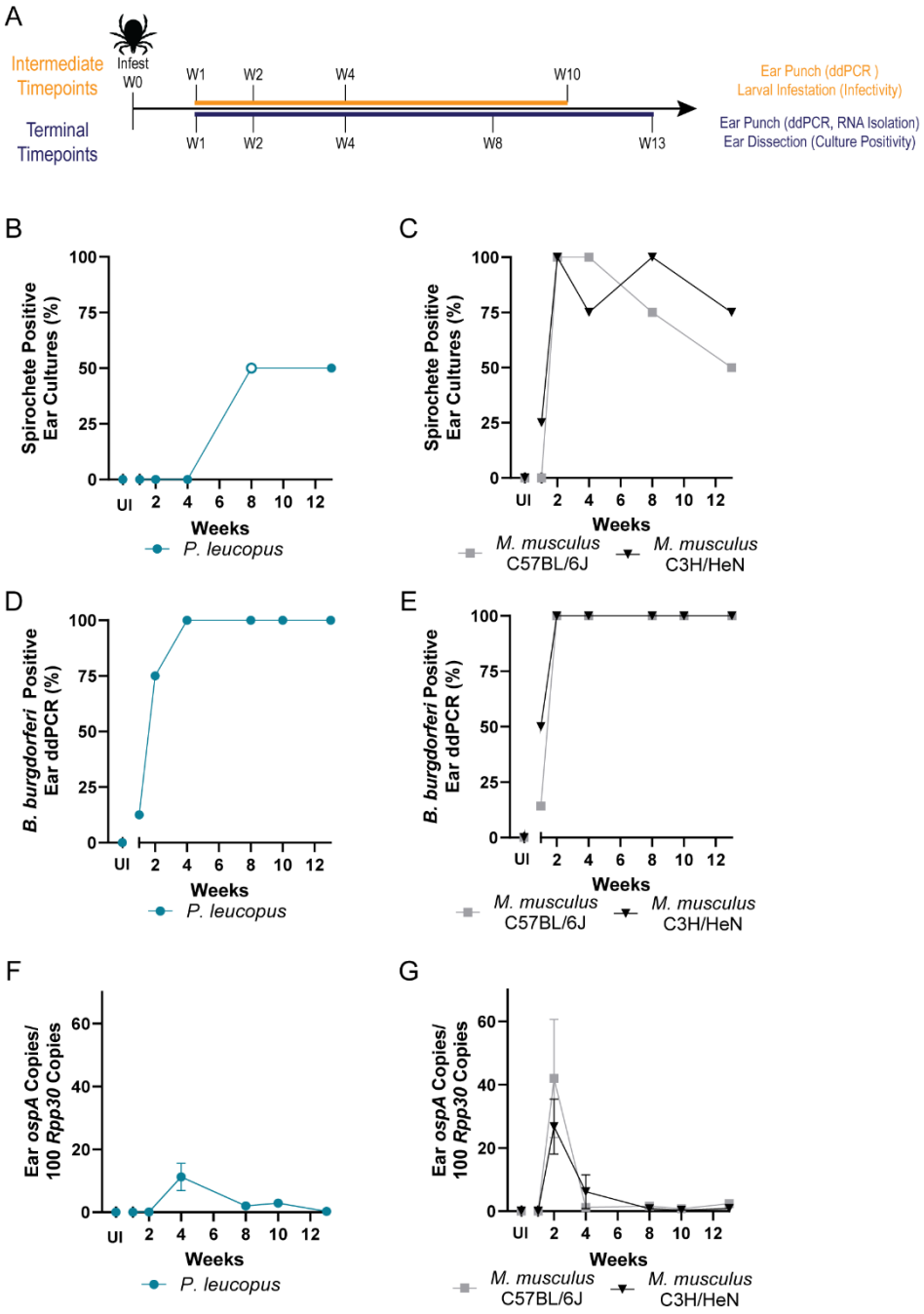

Figure 2: *B. burgdorferi* have different population dynamics in *P. leucopus* and *M. musculus* over thirteen weeks. (A) Schematic of the experimental design used for Figures 2-5. Rodents were infested with five nymphal ticks (infected or uninfected) in a tick containment chamber and harvested at the listed terminal timepoints. Rodents were subjected to a maximum of one intermediate timepoint analysis. All

rodents were between 6 and 12 weeks old at the time of infection. Each timepoint included one male and one female rodent per species per experiment where possible. All timepoints represent between three and eight samples per summarized point depending on if the timepoint combines terminal and intermediate values and/or whether samples needed to be excluded for technical reasons (*e.g.* rodent death, failed DNA extraction). (B, C) *B. burgdorferi* can be cultured from *P. leucopus* ear punches late in infection (B), while *M. musculus* can be cultured from ear punches starting at two weeks post nymph placement (C). The open circle at eight weeks in panel B represents a contamination issue that prevented us from accurately determining positivity in two of our four cultures. Thus, the appropriate interpretation of this timepoint is that at least half the cultures were positive for spirochetes. (D,E) *B. burgdorferi* can be detected by ddPCR in *P. leucopus* (D) and *M. musculus* (E) ears for most of the infection. A threshold of 1 copy of *ospA* per 10,000 copies of *Rpp30* was selected to distinguish between positive and negative samples. (F,G) *B. burgdorferi* experiences different population kinetics by ddPCR in *P. leucopus* (F) and *M. musculus* (G) ears. Data are normalized to copies of the mammalian *Rpp30* gene. Dots represent the mean, error bars the standard error of the mean.

***P. leucopus* are infectious for a shorter period of time than *M. musculus*.**

As *P. leucopus* are one of the primary North American *B. burgdorferi* reservoirs [8], we hypothesized that despite low bacterial abundance in skin the rodents would still efficiently transmit the spirochete to larval ticks. To test this hypothesis, we infested rodents in our timecourse **(Figure 2A)** with larval ticks at intermediate timepoints. Notably, we also ear punched the rodents in order to calculate bacterial burden for each specific rodent at the time of infestation.

P. leucopus were infectious very soon after nymph placement with ~25% of larval ticks collected yielding viable *B. burgdorferi* within a week of nymph placement **(Figure 3A)**. This increased to 80% at two weeks post nymph placement before sequentially dropping for the duration of the experiment. Notably there was no correlation between the observed bacterial burden in the ear by ddPCR and the proportion of infected larvae recovered from the rodents **(Figure 3B)**. Curiously, we also did not observe a correlation between our ability to culture *B. burgdorferi* from *P. leucopus* **(Figure 3B)** and the proportion of infected larvae recovered. These data together may suggest that in addition to having smaller numbers of viable *B. burgdorferi* in skin, *P. leucopus* may have additional mechanisms to inhibit the spread of *B. burgdorferi* to ticks.

Examining rodent-to-tick transmission in lab mice revealed a substantially different pattern. In C57BL/6J mice ~70% of larvae became infected when placed one week after nymph placement, 100% were infected when placed after two weeks, and >90% were infected when placed thereafter **(Figure 3C**). Similar to *P. leucopus*, there was no relationship between the burden in ear and infectivity **(Figure 3D)**. Curiously, while C3H/HeN mice had very similar results to C57BL/6J mice in terms of infectivity kinetics **(Figure 3E)**, we did actually observe a correlation between the burden in ear and infectivity ($p=0.001$, $R^2=0.5755$; Pearson Correlation). Curiously, this aligns with a recent study which found a relationship between skin burden and larval infectivity in C3H/HeJ mice [24]. Regardless, these data collectively demonstrate that the inbred *M. musculus* strains used here transmit to ticks better and over longer periods of time than a natural North American mammalian reservoir *P. leucopus*.

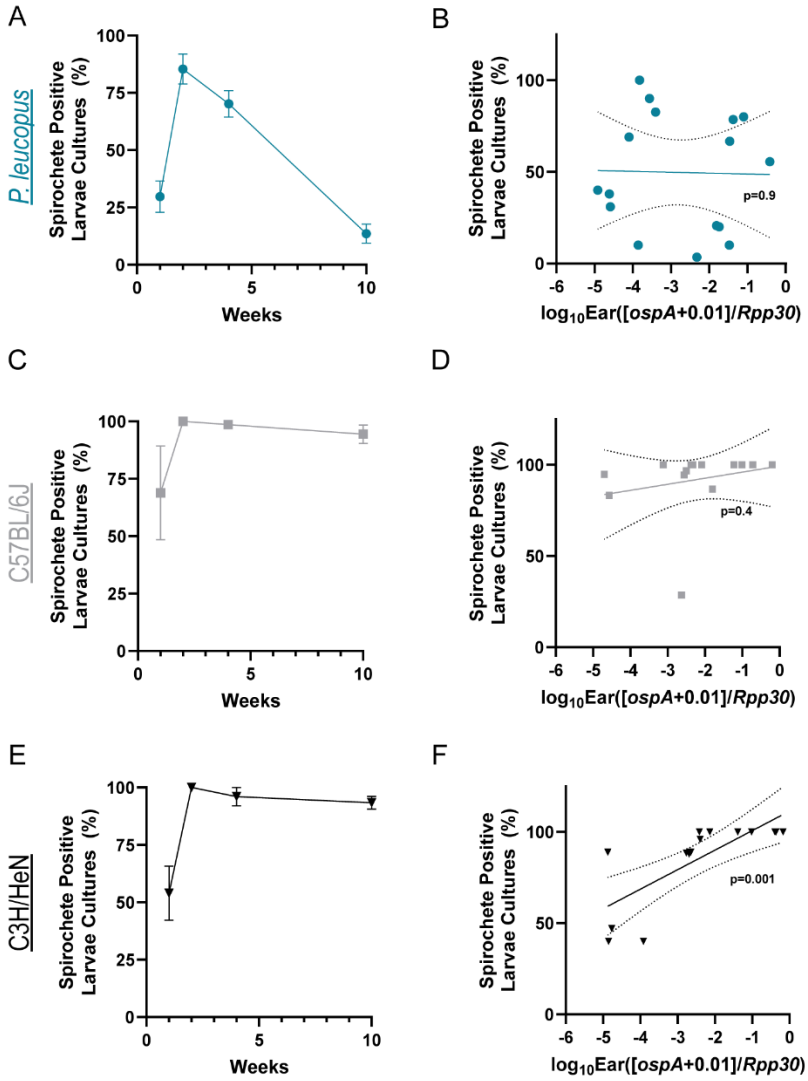

Figure 3: *P. leucopus*, but not *M. musculus*, become substantially less infectious over time. (A) *P. leucopus* are less infectious over time. Rodents were infested with approximately 50 larval *I. scapularis* at the time points listed. Larvae were collected 3-4 days later and incubated at room temperature in a humidified chamber for one week before being crushed in BSK-II. Cultures were monitored for three weeks to determine the rate of infectivity from the rodents to *I. scapularis.* (B) *B. burgdorferi* burden by ddPCR does not correlate with *P. leucopus* infectivity. Ear punches were taken just before infestation with larval ticks. (C, D) C57BL/6J mice remain highly infectious over time (C) and burden by ddPCR does not correlate with infectivity (D). (E,F) C3H/HeN mice remain highly infectious over time (E) and burden by ddPCR does correlate with infectivity (F). For panels A, C, D the number of ticks that yielded spirochetes was divided by the total number of ticks collected (5-30 ticks per rodent were collected, average=20.5 ticks/rodent). Rodents with fewer than 5 ticks collected were excluded. Each dot is the mean of 3-4 rodents and the error bar is the standard error of the mean. For panels B, D, F each dot is an individual rodent, the error bars mark the 95% confidence interval of the slope, and the p-value is from a Pearson r correlation.

P. leucopus skin transcriptomics reveal a subtle but prolonged immune response against *B. burgdorferi*.

We hypothesized that our findings that *B. burgdorferi* have an impaired ability to reach high bacterial burdens in skin and transmit to ticks in *P. leucopus* could be the result of the rodent having a subtle but efficient immune response that limits the pathogen's fitness. To test this hypothesis, we performed RNA-seq on *P. leucopus* ear tissue from 1-, 2-, 4-, and 8-weeks post infestation. Notably, while bulk RNA-seq is a blunt tool which cannot always capture the complexities of an immune response, it is a very useful technique to begin probing *P. leucopus* immunity given the very small number of validated antibody and other molecular tools for the species.

Differential expression analysis identified a small number of upregulated and downregulated genes across timepoints **(Figure 4A-D, Supplemental File 1)**. Because we sought to understand *P. leucopus* pathway regulation in response to *B. burgdorferi* we decided to use a less stringent statistical threshold ($p \leq 0.01$) in order to reduce our false negative hit rate. This analysis revealed 10 differentially expressed genes at one week post infestation, 138 at two weeks, 35 at four weeks, and 26 at eight weeks **(Figure 4E)**. Curiously, most of these genes had increased expression in response to infection, in line with activation of an immune response. Tracking these differentially expressed genes across infection revealed that most genes upregulated at two weeks post infestation did not remain upregulated later during infection **(Figure 4F**). However, many of the genes that were still overexpressed at four weeks post infestation also had high expression at eight weeks. Thus, it appears, after a burst of transcriptomic changes in skin by *P. leucopus* during acute infection, the transcriptomic response to *B. burgdorferi* is refined and sustained into late infection. This level of overlap across timepoints is not observed across downregulated genes **(Figure 4G)**.

Analysis of individual differentially expressed genes revealed a number of interesting observations. First, across two weeks, four weeks, and eight weeks post infestation we observed upregulation of multiple C1q genes, which could lead to increased complement-mediated killing of *B. burgdorferi* at these timepoints. Additionally, we observed high expression of *Cxcl13* at four weeks and eight weeks post infestation, which may suggest resident cells are recruiting additional B cells to the skin to kill invading *B. burgdorferi*. Finally, we observed highly statistically significant ($p_{adj} \approx 10^{-60}$) increased expression of *Slamf9* at four weeks and eight weeks post infestation. Notably, this gene was also one of the top hits from Long *et al.*'s study examining *P. leucopus* differential skin expression at five weeks post IP *B. burgdorferi* infection [14]. *Slamf9* has been associated with proinflammatory cytokine secretion in macrophages [25] and dendritic cells [26]. This may suggest a role for these cells in mediating late-stage inflammation against *B. burgdorferi* in skin.

We next utilized the Qiagen Ingenuity Pathway Analysis (IPA) pipeline [27] to understand which biological pathways appear to be differentially regulated in *P. leucopus* in response to *B. burgdorferi*. Critically, the pathways tested by these tools are based on signaling pathways in mice, which may differ from pathways in *P. leucopus*. Understanding this caveat, we used this tool and identified enrichment of differentially expressed genes in numerous canonical pathways associated with immunity **(Figure 4H)**, including phagocytosis, complement, macrophage activity, and B cell & T cell functions at two weeks, four weeks, and eight weeks post infestation. Notably, none of these pathways were enriched in differentially expressed genes at one week post infestation. The analysis also identified numerous cytokine induced pathways (including IL6, TNF, OSM, and IL1β) that were enriched in the two week, four week, and/or eight week datasets

(Figure 4I), as well as some immunity associated transcription factor pathways (including STAT3, NFKB2, and STAT5B) that were enriched in some combination of the datasets **(Figure 4J)**. Note, this does not mean that the cytokine or transcription factor itself is differentially regulated in our dataset, but rather that genes known to be regulated by those upstream regulators are enriched in our dataset. Importantly, the IPA pipeline not only assigns a P-value for enrichment, but also attempts to leverage the direction of effect for each differentially expressed gene to determine whether the predicted pathway is turned on or off. Because of the low number of differentially expressed genes at weeks four and eight this software was unable to generate Z scores for most pathways at these timepoints, however, even with these limitations the software was able to detect evidence of activated phagosome formation pathways at two weeks, four weeks, and eight weeks **(Figure 4K)**, indicating a strong signal of elevated phagocyte populations in skin following *B. burgdorferi* infection.

Focusing on the two-week timepoint where we see a stronger acute response to *B. burgdorferi*, the IPA software was able to detect activation of a number of immune-relevant pathways including phagosome formation, phagocytosis, pathogen recognition receptor activation, NK cell activation, and IL10 signaling **(Figure 4L)**. Examining activation of cytokine triggered pathways, the software detected strong activation of TNF and OSM pathways, and near significant activation of the IFNγ pathway (Z score = 1.97) **(Figure 4M)**. Curiously, by this analysis IL10 was not predicted to be significantly active. Finally, examining transcription factor activated pathways the software found evidence of activation of the T cell transcription factor BHLHE40, STAT3, the proinflammatory macrophage transcription factor KLF6, and STAT5B **(Figure 4N)**. The software predicted significant repression of the CEBPB and DLX3 regulated pathways. Together, these data demonstrate that while we observe a small number of differentially expressed genes in skin following *B. burgdorferi* infection, these genes provide a strong signature of an innate and adaptive immune response against the pathogen.

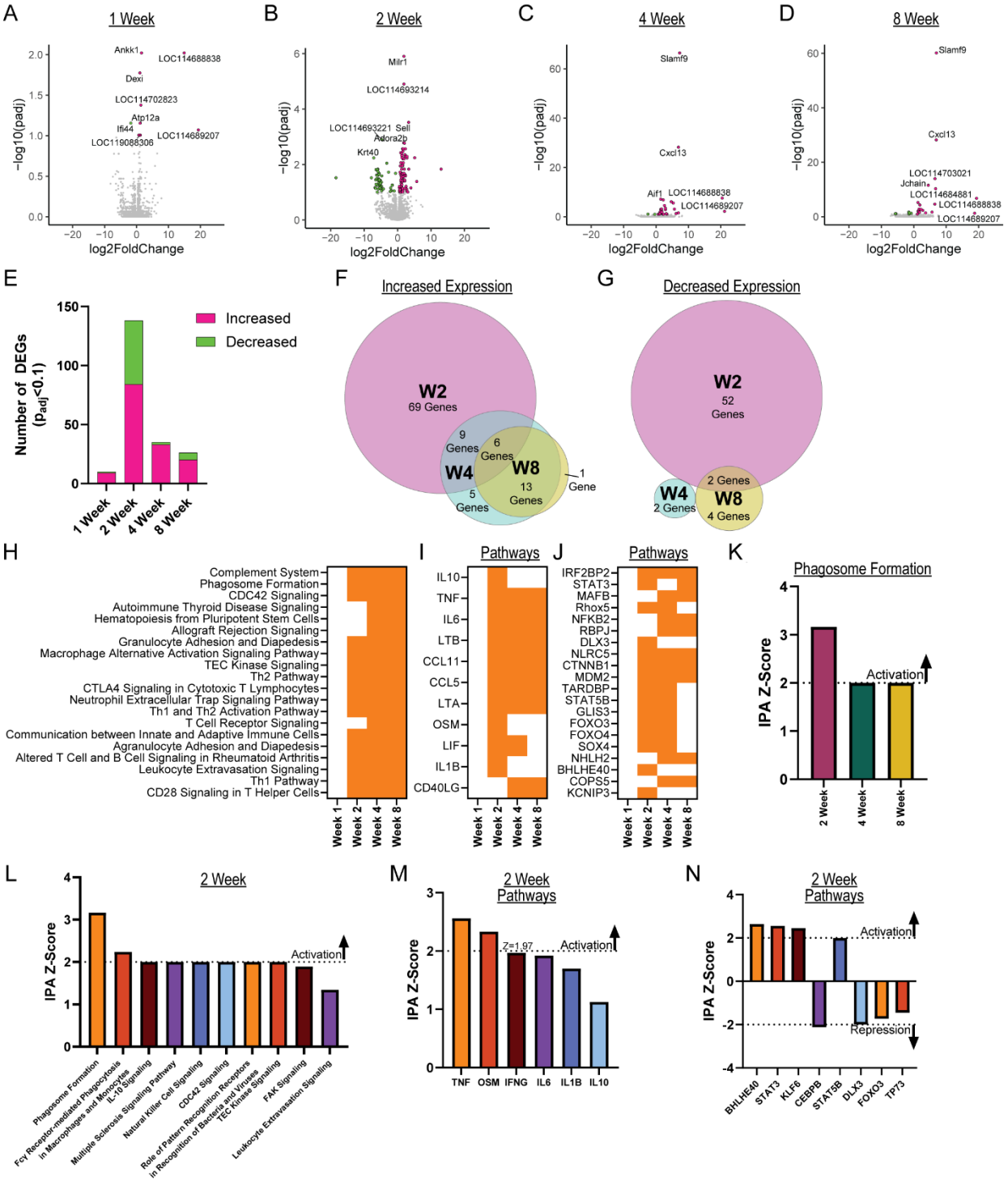

Figure 4: *P. leucopus* have a subtle but prolonged immune response to *B. burgdorferi* in skin. (A-D) Differentially expressed genes in *P. leucopus* skin at 1- (A), 2- (B), 4- (C), and 8-weeks (D) post infestation compared to uninfected *P. leucopus*. Genes with p<0.1 are colored green or pink if down or up regulated, accordingly. (E) More genes are upregulated than downregulated across timepoints using a p<0.1 threshold. (F, G) Many upregulated genes (F) but not downregulated genes (G) overlap across timepoints. Overlap between gene sets was determined using the Biovenn software [28]. (H-N) QIAGEN IPA software [27] reveals enrichment of numerous inflammatory pathways in *B. burgdorferi* infected *P. leucopus*. (H-I)

Heatmaps show pathways with enrichment for numerous canonical pathways (H) and upstream cytokine (I) and transcription factor (J) regulators. Orange boxes represent pathways where enrichment was predicted ($p<0.05$). (K) *P. leucopus* ears at 2-, 4-, and 8-weeks post infestation show activation of phagosome formation pathways. (L-N) At two weeks post infestation *P. leucopus* ears show evidence of activation of canonical pathways (L), activation of cytokine-triggered pathways (M), and activation & repression of transcription factor-regulated pathways (N). For K-N, activation of pathways was determined using a Z score cutoff of 2 and repression was determined using a Z score cutoff of -2. RNA was derived from 4 *P. leucopus* (two males, two females) at each timepoint.

Discussion

A primary goal of this work was not only to understand (a) how *P. leucopus* respond to *B. burgdorferi,* but (b) how this response compares to the traditional *M. musculus* lab mouse model of infection. Historically, the lab mouse has been used simultaneously to model manifestations of human Lyme disease and a catch all model of mammalian-*B. burgdorferi*-tick infection kinetics. However, our data suggest that *M. musculus* are a reasonably poor mimic of *P. leucopus*-*B. burgdorferi* interactions, as *B. burgdorferi* are not able to reach the same burdens in *P. leucopus* as *M. musculus*, are more difficult to culture from *P. leucopus*, and have reduced capacity to infect larval *I. scapularis*. While *M. musculus* and muroids can serve as competent hosts for *B. burgdorferi*—particularly in Europe—North American *B. burgdorferi* strains predominantly coexist with *P. leucopus* and shrews [8], and thus we were surprised to observe this elevated fitness in the non-native host.

We have three non-mutually exclusive explanations for these unintuitive observations. First, it is possible that *B. burgdorferi* is not under selection to reach high levels of infection or infectivity in nature, as the sheer number of *P. leucopus* and *I. scapularis* in North America mean even a mildly successful mammalian infection results in reproductive success from the bacteria's perspective. Given the number of selective pressures *B. burgdorferi* faces across the enzootic cycle, including cycling into and out of a range of vertebrate hosts beyond *P. leucopus*, it's possible that this represents a "hedged" strategy in which *B. burgdorferi* can infect numerous hosts to various degrees while selection ensures only that the spirochete remains at least partially infectious in the *P. leucopus* host. This is supported by data that the *ospC* genotype (Genotype A) in B31 is associated with a generalist lifestyle [29, 30]. Second, while the peaks of nymphal and larval *I. scapularis* density are often represented as being separated by seasons (~1-3 months depending on site), there is a range of time where both larvae and nymphs can be found in the environment [21-23]. As an extreme example, co-feeding can even be observed during spring field studies—likely due to larvae that persisted from the previous fall. Therefore, it's possible that most *P. leucopus* to *I. scapularis* larvae transmission occurs during the first month of infection when we still observe high rates of infectivity. While these two hypotheses may explain the lower-than-expected *P. leucopus* infectivity, they do not explain the higher-than-expected fitness in the non-native host *M. musculus.* Our third explanation is therefore that the specific *M. musculus* strains selected here may be uniquely permissive to *B. burgdorferi* zoonosis. To address this, future work will examine *B. burgdorferi* fitness in outbred murine hosts. Additionally, as there are approximately 25 million years of divergent evolution between *P. leucopus* and *M. musculus* [31], it may also be interesting to compare *P. leucopus* with a more closely-related model organism such as hamsters to better examine how unique the relationship is between *P. leucopus* and *B. burgdorferi*.

In this work and in a past transcriptomic study [14] we note limited direct evidence of immunity (*e.g.* a large number of differentially expressed cytokines), which can likely be attributed to the relatively small number of infiltrating immune cells into the large numbers of epithelial and mesenchymal cells that make up the tissue. However, based on our data examining *B. burgdorferi* fitness during the acute stages of *P. leucopus* infection, we hypothesize that the immune response we detect here is extremely efficient and contributes to limiting *B. burgdorferi* zoonosis. Curiously, while we observed overlap of increased *Slamf9* expression in *B. burgdorferi* infected *P. leucopus*, this represents one of only a few similarities between our work and the Long *et al*. dataset [14]. We note numerous differences in the experimental design that may account for differences between the studies: (1) differences in infection method (IP vs Nymph), (2) differences in *B. burgdorferi* strain (Sh-2-82 vs B31), and (3) differences in *P. leucopus* source (LL Stock from the Peromyscus Genetic Stock Center vs the Tufts University Peromyscus Colony). Dissecting the impacts of these variables on *P. leucopus*-*B. burgdorferi* interactions remains an important future direction. Current work is also focused on comparing and contrasting the differentially expressed genes in *P. leucopus* skin following infection to those that are differentially expressed in *M. musculus*. For instance, comparing our dataset to a single cell RNA-sequencing dataset generated on C57BL/6J ankles (Helble *et al*. accepted) revealed that while we observe high *Cxcl13* expression late in infection in *P. leucopus* skin, it is associated only with early infection in *M. musculus* ankles. Further mining of these datasets may provide insight into why *M. musculus*, but not *P. leucopus,* remain infectious to larval ticks over long periods of time.

We note that we are not the first group to attempt to measure experimentally infected *P. leucopus* transmission of *B. burgdorferi* to *I. scapularis*, and indeed our measurements of infectivity align with prior observations using the JD1 strain of *B. burgdorferi* [16], but curiously diverged substantially from a recent report which used the B31-5A4 clonal strain and found larval infectivity increased over the first five weeks of infection before slightly dropping eight weeks post infection [32]. We note that in this latter report qPCR was used to detect *B. burgdorferi* rather than culture-based methods used here. We speculate that the use of PCR may have overreported the abundance of infected ticks, as DNA can persist without the presence of viable *B. burgdorferi*. This pairs well with our finding that we could not correlate *B. burgdorferi* fitness in skin (either by ddPCR or culture positivity) with rates of transmission in *P. leucopus*, which together lead us to hypothesize that there are soluble mechanisms of diminishing transmission to ticks via the bloodmeal in *P. leucopus*. This finding may partly explain why field studies often find that, on average, approximately 15-25% of *I. scapularis* are infected with *B. burgdorferi* in endemic regions [33] despite much higher rates of *P. leucopus* infection [9]. Importantly, ecological explanations including larval ticks feeding on a wide range of hosts [8] likely have substantial impacts on this statistic.

A major limitation and important future direction of this work is that we only tested our findings with the B31 *B. burgdorferi* strain. We chose B31 (originally derived from a North American tick [34]) because it is the most commonly used laboratory strain and the genomic type strain of *B. burgdorferi* and as such, our results would be comparable to other studies using this strain in mice. Recent work has highlighted that there are bacterial strain dependent differences in the ability for *B. burgdorferi* to transmit from C3H/HeJ mice to *I. scapularis* [24], raising the possibility that other strains may be better or worse adapted to *P. leucopus*. In line with this, there is some evidence of strain specificity within different reservoir hosts [29, 32, 35], despite *B. burgdorferi*'s reputation as a generalist. Screening additional strains in *P. leucopus* could enable

identification of variable loci that associate with higher transmission. Understanding the impacts of those theoretical loci on spread from other vertebrate hosts and impacts on clinical manifestations of Lyme disease could broaden our understanding of *B. burgdorferi* evolution.

In sum, our data demonstrate that the infection, spread, and control of *B. burgdorferi* follow dramatically different rules in *P. leucopus* than we observe in *M. musculus*. This highlights a tried-and-true principal of experimental design borrowed from the statistician George E. P. Box: "All models are wrong, but some are useful." Here we propose that while *M. musculus* are a useful model for many aspects of *B. burgdorferi* infection, they may not accurately model the North American enzootic cycle. We hope that improving our understanding of how *P. leucopus* resist *B. burgdorferi* infection could provide new insights into controlling *B. burgdorferi* abundance in nature through reservoir targeted interventions.

Acknowledgements
The authors would like to thank Dr. Alan Barbour for numerous helpful conversations over the course of this project. RNA sequencing analyses were made possible by the Tufts High Performance Computing Cluster (https://it.tufts.edu/high-performance-computing). We thank past and present members of the Hu lab for helpful feedback during the formulation of this project and in assisting with the bioinformatic analyses, particularly Julie McCarthy and Peter Gwynne.

Methods

Bacterial culture

Borrelia burgdorferi strain B31 were propagated in Barbour-Stoenner-Kelley II (BSK-II) medium in stationary, sealed tubes at 32°C until mid-exponential phase growth (~$5x10^7$ spirochetes/mL). Bacteria were monitored for growth, motility, and counted by pairing a Petroff-Hausser counter with darkfield microscopy. B31 stocks were passaged once *in vitro* following isolation from subcutaneously infected C3H/HeJ (Jackson Labs, Strain: 000659) skin two to four weeks post-infection in order to generate frozen stocks in 25% glycerol. Plasmid content was measured after thawing from frozen stocks. In order to limit environmental contamination when culturing spirochetes from rodent or tick tissue phosphomycin (100µg/mL), rifampicin (50µg/mL), and amphotericin B (5µg/mL) were added to the medium. Cultures from tissue were monitored weekly by darkfield microscopy and cultures were considered positive if spirochetes were observed within three weeks of culture start.

Rodent Maintenance, Use, and Ethical Statement

All animal procedures were approved by the Tufts University-Tufts Medical Center Institutional Animal Care and Use Committee (IACUC, Protocol #B2021-84). Euthanasia was performed in accordance with guidelines provided by the AVMA and was approved by the Tufts University IACUC. Rodents were maintained by the Tufts Comparative Medicine Services. Sex, age, and numbers of rodents used in each experiment are described in figure legends.

Generation of *Ixodes scapularis* Nymphs

Immunocompromised C3H *scid* mice (Jackson Labs, Strain: 001131) were infected by subcutaneous injection of $1x10^5$ *B. burgdorferi* in 200µL of BSK-II media. Two to eight weeks post-infection mice were infested with larval *I. scapularis* (National Tick Research and Education Resource, Oklahoma State University, stored at 4°C in airtight containers containing saturated

potassium sulfate). To infest mice, ~100 larval ticks were placed in modified 50mL conical tube prior to placing a mouse in the tube. Mice were restrained with ticks for one hour before returning to a cage suspended in a water moat. Water moats were monitored for ten days to collect fed larval ticks. Up to 6 fed ticks were stored in 1.7mL microcentrifuge tubes with needle-generated airholes in an airtight glass desiccator containing water. Ticks were aged between 10 and 52 weeks prior to use for infection. Uninfected ticks were identically generated except for the use of uninfected C57BL/6J (Jackson Labs, Strain: 000664) mice.

Rodent Infection with *B. burgdorferi*

Mus musculus (C57BL/6J [Jackson Labs, Strain: 000664], C3H/HeN [Charles River Laboratories, Strain: 025]) and *Peromyscus leucopus* (Sam Telford, Tufts University) were shaved prior to infection. The *P. leucopus* colony has been inbred since 1994 and have been maintained under specific pathogen-free conditions. For needle infections, 200µL of BSK-II containing $1x10^5$ bacteria were subcutaneously injected into each mouse. For nymph placements, a 1:4 mixture of melted beeswax to rosin gum mixture was heated and used to attach the top of a modified 1.7mL microcentrifuge tube lined with mesh between the shoulder blades of the rodent. Five nymphal ticks were carefully placed through the mesh and into the placement cap. Four days later, caps were carefully removed, and ticks were collected. Mice were singly housed in cages suspended in a water moat until all ticks were collected. Rodents were then returned to cohabitation with other infected animals of the same strain and sex.

Determining bacterial burden

DNA from ears was collected by taking 1-2 2mm ear punches from one or both ears at listed time points. DNA from the tick bite or needle site was collected by dissection of a roughly 2mm region in the center of the shaved region. In all cases, DNA was extracted using the Qiagen Blood and Tissue kit following overnight incubation at 56°C in Buffer ATL with Proteinase K. Following DNA extraction, digital droplet PCR (ddPCR) was performed to quantify the amount of *B. burgdorferi* DNA relative to rodent DNA. Primer probe pairs are listed in **Table 1**. Briefly, the Bio-Rad ddPCR Supermix for Probes (no dUTP) kit was used to perform the reaction within droplets generated by the QX200 droplet generator (Bio-Rad) in Oil-for-Probes (Bio-Rad). The reaction included 10 minutes at 95°C, 40 cycles of 94°C for 30 seconds and 60°C for 1 minute, followed by 10 minutes at 98°C and cooling to 4°C for at least 30 minutes to stabilize droplets. Fluorescence was calculated by the QX200 droplet reader and analyzed on the QX Manager Software (Bio-Rad).

Table 1: Oligonucleotides used in this study

Target	Forward	Reverse	Probe
Mus musculus Rpp30	CCAGCTCCGTTTGTGATAGT	CAAGGCAGAGATGCCCATAA	CTGTGCACACATGCATTTGAGAGGT (5'HEX, 3'Iowa Black FQ)
Peromyscus leucopus Rpp30	CTTAGCTCCCGCTTGTTTCT	AAACCTGGTAAGCCAGTGTC	ACACACTTTCTCCTCTTCTTGCTGCA (5'HEX, 3'Iowa Black FQ)
B. burgdorferi ospA	ATGTTAGCAGCCTTGACGAG	TCGTACTTGCCGTCTTTGTT	AGCGTTTCAGTAGATTTGCCTGGTG (5'6-FAM, 3'Iowa Black FQ)

RNA Extraction and Sequencing

One 2mm ear punches from each ear were collected and submerged in RNA-later (Invitrogen) overnight at room temperature before being frozen at -80°C. After all samples were collected, samples were thawed on ice, transferred to QIAzol, and bead beat with a 6.35mm chrome steel bead (Biospec Products) for two cycles of two minutes each at an oscillation frequency of 30/second using a TissueLyser II (Qiagen). RNA was extracted using the miRNeasy mini kit (Qiagen), with the modification that two RWT washes were performed. gDNA was digested using TURBO DNase (Invitrogen) and RNA was repurified using the RNeasy MinElute Cleanup Kit (Qiagen). Purified RNA were submitted to Azenta Life Sciences/Genewiz for library preparation and sequencing (Illumina HiSeq 2x150bp).

RNA Sequencing Analysis

Reads were aligned to the *P. leucopus* genome (GCF_004664715.2) [14] using STAR version 2.6.1 [36] and gene expression was summarized using RSEM version 1.3.1 [37]. All differential gene expression analyses were performed with R (version 4.3.1) using DESeq2 version 1.40.2 [38] using standard parameters. Only genes with ≥10 reads across all conditions (summed) were included in the analysis. Differential gene expression was calculated by comparing to uninfected rodents (rodents that were infested with uninfected nymphs and harvested one week later) and adjusted p-values were based off of a calculated false discovery rate. Additional pathway analysis was performed with the use of QIAGEN IPA (QIAGEN Inc., https://digitalinsights.qiagen.com/IPA) [27] using genes with an adjusted p-value cutoff of <0.1.

Determining Transmission from Rodents to Larval *Ixodes scapularis*

At each timepoint ~50 larval ticks were placed in modified 50mL conical tube prior to placing a mouse in the tube. Mice were restrained with ticks for one hour before returning to a cage suspended in a water moat. Water moats were monitored at days three and four to collect fed larval ticks. Between 5 and 30 fed larvae were collected per mouse and stored in an airtight glass desiccator containing water for one week to enable *B. burgdorferi* replication in the bloodmeal. Ticks were submerged in 70% ethanol and each tick was crushed in 1mL BSK-II containing phosphomycin (100µg/mL), rifampicin (50µg/mL), and amphotericin B (5µg/mL). Cultures were grown at 32°C, monitored weekly by darkfield microscopy, and cultures were considered positive if spirochetes were observed within three weeks of culture start.

Data Availability

Sequencing data are deposited in GEO under accession number GSE244071.

Citations

1. Steere, A.C., T.F. Broderick, and S.E. Malawista, *Erythema chronicum migrans and Lyme arthritis: epidemiologic evidence for a tick vector.* Am J Epidemiol, 1978. **108**(4): p. 312-21.
2. Wallis, R.C., et al., *Erythema chronicum migrans and lyme arthritis: field study of ticks.* Am J Epidemiol, 1978. **108**(4): p. 322-7.
3. Burgdorfer, W., et al., *Lyme disease-a tick-borne spirochetosis?* Science, 1982. **216**(4552): p. 1317-9.
4. Radolf, J.D., et al., *Of ticks, mice and men: understanding the dual-host lifestyle of Lyme disease spirochaetes.* Nat Rev Microbiol, 2012. **10**(2): p. 87-99.
5. Anderson, J.F., et al., *Involvement of birds in the epidemiology of the Lyme disease agent Borrelia burgdorferi.* Infect Immun, 1986. **51**(2): p. 394-6.
6. Kornblatt, A.N., P.H. Urband, and A.C. Steere, *Arthritis caused by Borrelia burgdorferi in dogs.* J Am Vet Med Assoc, 1985. **186**(9): p. 960-4.
7. Levine, J.F., M.L. Wilson, and A. Spielman, *Mice as reservoirs of the Lyme disease spirochete.* Am J Trop Med Hyg, 1985. **34**(2): p. 355-60.
8. Goethert, H.K., et al., *Host-utilization differences between larval and nymphal deer ticks in northeastern U.S. sites enzootic for Borrelia burgdorferi sensu stricto.* Ticks Tick Borne Dis, 2023. **14**(6): p. 102230.
9. Bunikis, J., et al., *Borrelia burgdorferi infection in a natural population of Peromyscus Leucopus mice: a longitudinal study in an area where Lyme Borreliosis is highly endemic.* J Infect Dis, 2004. **189**(8): p. 1515-23.
10. Hofmeister, E.K., et al., *Longitudinal study of infection with Borrelia burgdorferi in a population of Peromyscus leucopus at a Lyme disease-enzootic site in Maryland.* Am J Trop Med Hyg, 1999. **60**(4): p. 598-609.
11. Moody, K.D., et al., *Experimental Borrelia burgdorferi infection in Peromyscus leucopus.* J Wildl Dis, 1994. **30**(2): p. 155-61.
12. Wright, S.D. and S.W. Nielsen, *Experimental infection of the white-footed mouse with Borrelia burgdorferi.* Am J Vet Res, 1990. **51**(12): p. 1980-7.
13. Schwanz, L.E., et al., *Borrelia burgdorferi has minimal impact on the Lyme disease reservoir host Peromyscus leucopus.* Vector Borne Zoonotic Dis, 2011. **11**(2): p. 117-24.
14. Long, A.D., et al., *The genome of Peromyscus leucopus, natural host for Lyme disease and other emerging infections.* Sci Adv, 2019. **5**(7): p. eaaw6441.
15. Gaber, A.M., et al., *Comparative transcriptome analysis of Peromyscus leucopus and C3H mice infected with the Lyme disease pathogen.* Front Cell Infect Microbiol, 2023. **13**: p. 1115350.
16. Donahue, J.G., J. Piesman, and A. Spielman, *Reservoir competence of white-footed mice for Lyme disease spirochetes.* Am J Trop Med Hyg, 1987. **36**(1): p. 92-6.
17. Trager, W., *Living Together The Biology of Animal Parasitism*. 1986, New York: Springer New York.
18. Balderrama-Gutierrez, G., et al., *An Infection-Tolerant Mammalian Reservoir for Several Zoonotic Agents Broadly Counters the Inflammatory Effects of Endotoxin.* mBio, 2021. **12**(2).
19. Ana Milovic, J.V.D., Alan G. Barbour, *The white-footed deermouse, an infection tolerant reservoir for several zoonotic agents, tempers interferon responses to endotoxin in comparison to the mouse and rat.* eLife, 2023. **12**(RP90135).
20. Ma, Y., et al., *Distinct characteristics of resistance to Borrelia burgdorferi-induced arthritis in C57BL/6N mice.* Infect Immun, 1998. **66**(1): p. 161-8.

21. Simmons, T.W., et al., *Seasonal Activity, Density, and Collection Efficiency of the Blacklegged Tick (Ixodes scapularis) (Acari: Ixodidae) in Mid-Western Pennsylvania.* J Med Entomol, 2015. **52**(6): p. 1260-9.
22. Han, S., et al., *Seasonality of acarological risk of exposure to Borrelia miyamotoi from questing life stages of Ixodes scapularis collected from Wisconsin and Massachusetts, USA.* Ticks Tick Borne Dis, 2021. **12**(1): p. 101556.
23. Ogden, N.H., et al., *Evidence for Geographic Variation in Life-Cycle Processes Affecting Phenology of the Lyme Disease Vector Ixodes scapularis (Acari: Ixodidae) in the United States.* J Med Entomol, 2018. **55**(6): p. 1386-1401.
24. Zinck, C.B., et al., *Variation among strains of Borrelia burgdorferi in host tissue abundance and lifetime transmission determine the population strain structure in nature.* PLoS Pathog, 2023. **19**(8): p. e1011572.
25. Dollt, C., et al., *The novel immunoglobulin super family receptor SLAMF9 identified in TAM of murine and human melanoma influences pro-inflammatory cytokine secretion and migration.* Cell Death Dis, 2018. **9**(10): p. 939.
26. Shachar, I., et al., *SLAMF receptors on normal and malignant B cells.* Clin Immunol, 2019. **204**: p. 23-30.
27. Kramer, A., et al., *Causal analysis approaches in Ingenuity Pathway Analysis.* Bioinformatics, 2014. **30**(4): p. 523-30.
28. Hulsen, T., J. de Vlieg, and W. Alkema, *BioVenn - a web application for the comparison and visualization of biological lists using area-proportional Venn diagrams.* BMC Genomics, 2008. **9**: p. 488.
29. Combs, M.A., et al., *Host adaptation drives genetic diversity in a vector-borne disease system.* PNAS Nexus, 2023. **2**(8): p. pgad234.
30. Earnhart, C.G., et al., *Demonstration of OspC type diversity in invasive human lyme disease isolates and identification of previously uncharacterized epitopes that define the specificity of the OspC murine antibody response.* Infect Immun, 2005. **73**(12): p. 7869-77.
31. Steppan, S., R. Adkins, and J. Anderson, *Phylogeny and divergence-date estimates of rapid radiations in muroid rodents based on multiple nuclear genes.* Syst Biol, 2004. **53**(4): p. 533-53.
32. Lin, Y.P., et al., *Cellular and immunological mechanisms influence host-adapted phenotypes in a vector-borne microparasite.* Proc Biol Sci, 2022. **289**(1969): p. 20212087.
33. Foster, E., et al., *Prevalence of five human pathogens in host-seeking Ixodes scapularis and Ixodes pacificus by region, state, and county in the contiguous United States generated through national tick surveillance.* Ticks Tick Borne Dis, 2023. **14**(6): p. 102250.
34. Johnson, R.C., et al., *Borrelia burgdorferi sp. nov.: Etiologic Agent of Lyme Disease.* International Journal of Systematic and Evolutionary Microbiology, 1984. **34**(4): p. 496-497.
35. Marcinkiewicz, A.L., et al., *Structural evolution of an immune evasion determinant shapes pathogen host tropism.* Proc Natl Acad Sci U S A, 2023. **120**(27): p. e2301549120.
36. Dobin, A., et al., *STAR: ultrafast universal RNA-seq aligner.* Bioinformatics, 2013. **29**(1): p. 15-21.
37. Li, B. and C.N. Dewey, *RSEM: accurate transcript quantification from RNA-Seq data with or without a reference genome.* BMC Bioinformatics, 2011. **12**: p. 323.
38. Love, M.I., W. Huber, and S. Anders, *Moderated estimation of fold change and dispersion for RNA-seq data with DESeq2.* Genome Biol, 2014. **15**(12): p. 550.